

Journal of The American Society for
MASS SPECTROMETRY



November 2017 / Volume 28 / Number 11 **Table of Contents**

ASMS NEWS & VIEWS

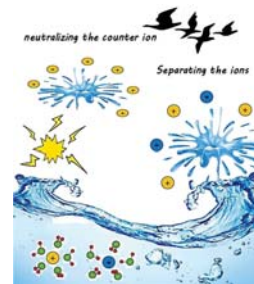
i-iii

ASMS News & Views
Edited by Gavin Reid

CRITICAL INSIGHT

2255–2261

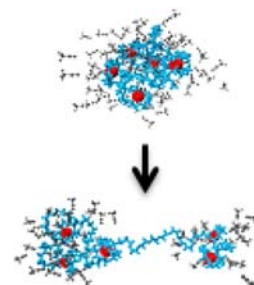
Transferring Ions from Solution to the Gas Phase:
The Two Basic Principles
S.F. Teunissen and M.N. Eberlin



RESEARCH ARTICLES

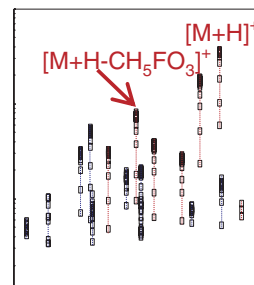
2262–2279

Charging and Release Mechanisms of Flexible Macromolecules
in Droplets
M.I. Oh and S. Consta



2280–2287

Extending a Tandem Mass Spectral Library to Include MS^2
Spectra of Fragment Ions Produced In-Source and MS^n Spectra
X. Yang, P. Neta, and S.E. Stein



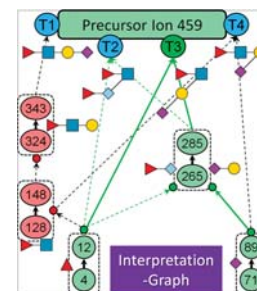
Instructions for authors for *The Journal of The American Society for Mass Spectrometry* can be found at
www.springer.com/13361

Abstracted/Index in: Academic OneFile, Academic Search, Chimica, CSA/Proquest, Current Abstracts, Current Contents/Physical, Chemical and Earth Sciences, EI-Compendex, EMBASE, Food Science and Technology Abstracts, Google Scholar, IBIDS, INIS Atomindex, Inspec, OCLC, PubMed/Medline, Science Citation Index, Science Citation Index Expanded (SciSearch), SCOPUS, and Summon by Serial Solutions.

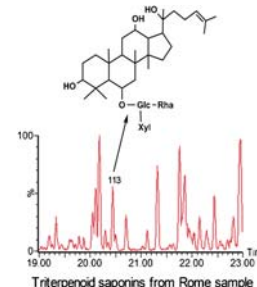
Journal of the American Society for Mass Spectrometry (ISSN 1044-0305) is published monthly by Springer Science & Business Media, 233 Spring St, 6th Fl., New York, NY. Periodicals postage is pending at New York, NY and additional mailing offices. POSTMASTER: Send address changes to *Journal of The American Society for Mass Spectrometry*, Springer, 233 Spring Street, New York, NY 10013, USA.

2288–2301

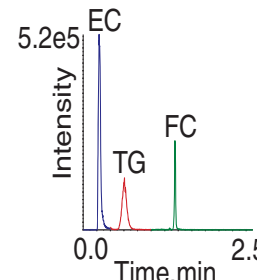
GlycoDeNovo – an Efficient Algorithm for Accurate de novo Glycan Topology Reconstruction from Tandem Mass Spectra
P. Hong, H. Sun, L. Sha, Y. Pu, K. Khatri, X. Yu, Y. Tang, and C. Lin

**2302–2318**

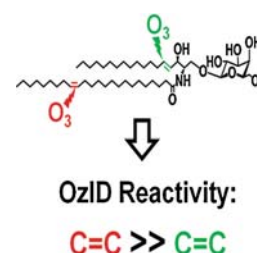
Rapid Characterization of Constituents in *Tribulus terrestris* from Different Habitats by UHPLC/Q-TOF MS
W. Zheng, F. Wang, Y. Zhao, X. Sun, L. Kang, Z. Fan, L. Qiao, R. Yan, S. Liu, and B. Ma

**2319–2329**

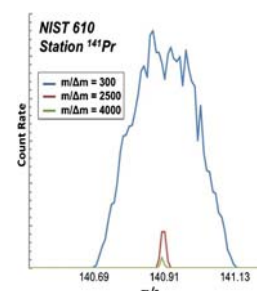
Simultaneous Quantification of Free Cholesterol, Cholesteryl Esters, and Triglycerides without Ester Hydrolysis by UHPLC Separation and In-Source Collision Induced Dissociation Coupled MS/MS
M.S. Gardner, L.G. McWilliams, J.I. Jones, Z. Kuklenyik, J.L. Pirkle, and J.R. Barr

**2330–2343**

Structural Analysis of Unsaturated Glycosphingolipids Using Shotgun Ozone-Induced Dissociation Mass Spectrometry
R.C. Barrientos, N. Vu, and Q. Zhang

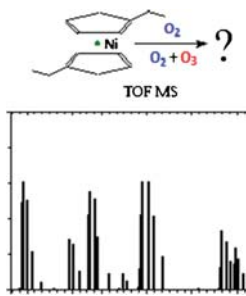
**2344–2351**

Improved Precision and Accuracy of Quantification of Rare Earth Element Abundances via Medium-Resolution LA-ICP-MS
R. Funderburg, R. Arevalo Jr., M. Locmelis, and T. Adachi

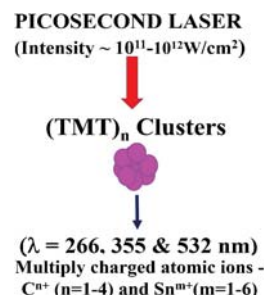


2352–2360

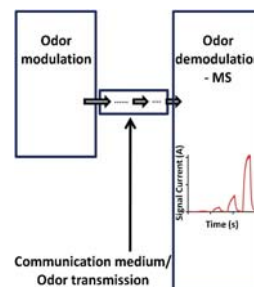
TOF MS Investigation of Nickel Oxide CVD
A.S. Kondrateva, M.V. Mishin, and S.E. Alexandrov

**2361–2370**

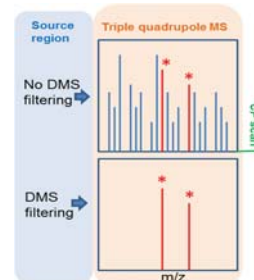
Tailoring Ion Charge State Distribution in Tetramethyltin Clusters under Influence of Moderate Intensity Picosecond Laser Pulse: Role of Laser Wavelength and Rate of Energy Deposition
P. Sharma, S. Das, and R.K. Vatsa

**2371–2383**

Molecular Communication over Gas Stream Channels using Portable Mass Spectrometry Samples
S. Giannoukos, A. Marshall, S. Taylor, and J. Smith

**2384–2392**

On the Nature of Mass Spectrometer Analyzer Contamination
Y. Kang, B.B. Schneider, and T.R. Covey

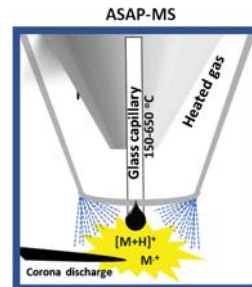
**2393–2400**

Rapid Analysis of Ingredients in Cream Using Ultrasonic Mist-Direct Analysis in Real-Time Time-of-Flight Mass Spectrometry
H. Shimada, K. Maeno, K. Kinoshita, and Y. Shida

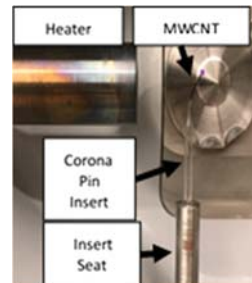


2401–2407

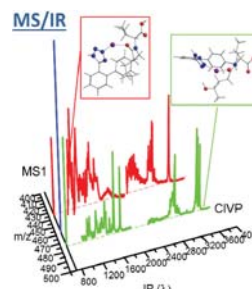
Application of Atmospheric Solids Analysis Probe Mass Spectrometry (ASAP-MS) in Petroleomics: Analysis of Condensed Aromatics Standards, Crude Oil, and Paraffinic Fraction
L.V. Tose, M. Murgu, B.G. Vaz, and W. Romão

**2408–2413**

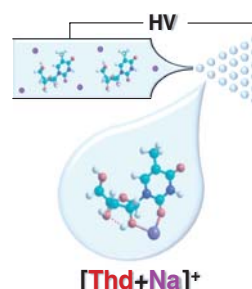
Carbon Nanotube Fiber Ionization Mass Spectrometry: A Fundamental Study of a Multi-Walled Carbon Nanotube Functionalized Corona Discharge Pin for Polycyclic Aromatic Hydrocarbons Analysis
K.S. Nahan, N. Alvarez, V. Shanov, and A. Vonderheide

**2414–2422**

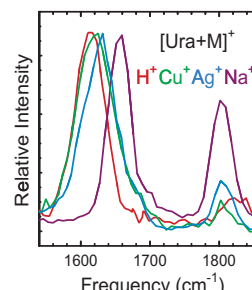
Identification and Partial Structural Characterization of Mass Isolated Valsartan and Its Metabolite with Messenger Tagging Vibrational Spectroscopy
O. Gorlova, S.M. Colvin, A. Brathwaite, F.S. Menges, S.M. Craig, S.J. Miller, and M.A. Johnson

**2423–2437**

IRMPD Action Spectroscopy, ER-CID Experiments, and Theoretical Studies of Sodium Cationized Thymidine and 5-Methyluridine: Kinetic Trapping During the ESI Desolvation Process Preserves the Solution Structure of [Thd+Na]⁺
Y. Zhu, H.A. Roy, N.A. Cunningham, S.F. Stroehn, J. Gao, M.U. Munshi, G. Berden, J. Oomens, and M.T. Rodgers

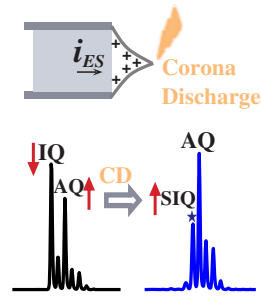
**2438–2453**

Influence of Transition Metal Cationization versus Sodium Cationization and Protonation on the Gas-Phase Tautomeric Conformations and Stability of Uracil: Application to [Ura+Cu]⁺ and [Ura+Ag]⁺
T.E. Akinyemi, R.R. Wu, Y.-W. Nei, N.A. Cunningham, H.A. Roy, J.D. Steill, G. Berden, J. Oomens, and M.T. Rodgers

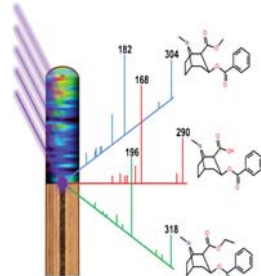


2454–2461

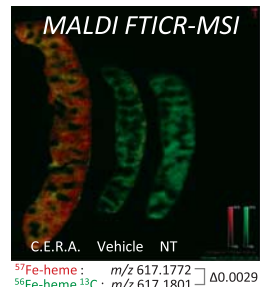
Unexpected Reduction of Iminoquinone and Quinone Derivatives in Positive Electrospray Ionization Mass Spectrometry and Possible Mechanism Exploration
J. Pei, C.-C. Hsu, R. Zhang, Y. Wang, K. Yu, and G. Huang

**2462–2468**

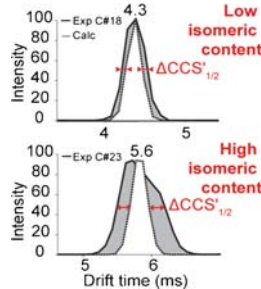
Optimization of Sample Preparation and Instrumental Parameters for the Rapid Analysis of Drugs of Abuse in Hair samples by MALDI-MS/MS Imaging
B. Flinders, E. Beasley, R.M. Verlaan, E. Cuypers, S. Francese, T. Bassindale, M.R. Clench, and R.M.A. Heeren

**2469–2475**

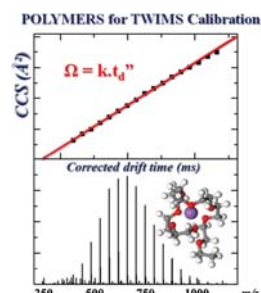
Visualization of ^{57}Fe -Labeled Heme Isotopic Fine Structure and Localization of Regions of Erythroblast Maturation in Mouse Spleen by MALDI FTICR-MS Imaging
M. Kihara, Y. Matsuo-Tezuka, M. Noguchi-Sasaki, K. Yorozu, M. Kurasawa, Y. Shimonaka, and M. Hirata

**2476–2482**

Effective Ion Mobility Peak Width as a New Isomeric Descriptor for the Untargeted Analysis of Complex Mixtures Using Ion Mobility-Mass Spectrometry
M. Farenc, B. Paupy, S. Marceau, E. Riches, C. Afonso, and P. Giusti

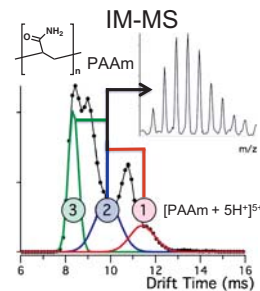
**2483–2491**

Polymers for Traveling Wave Ion Mobility Spectrometry Calibration
Q. Duez, F. Chirot, R. Liénard, T. Josse, C. Choi, O. Coulombier, P. Dugourd, J. Cornil, P. Gerbaux, and J. De Winter

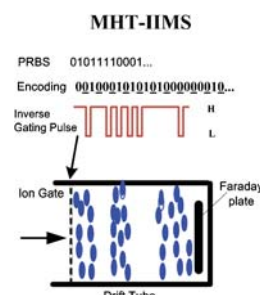


2492–2499

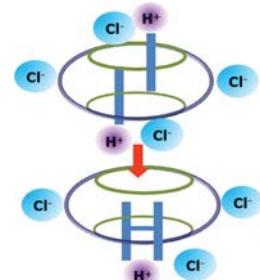
Multiple Gas-Phase Conformations of a Synthetic Linear Poly(acrylamide) Polymer Observed Using Ion Mobility-Mass Spectrometry
J.R.N. Haler, J. Far, A. Aqil, J. Claereboudt, N. Tomczyk, K. Giles, C. Jérôme, and E. De Pauw

**2500–2507**

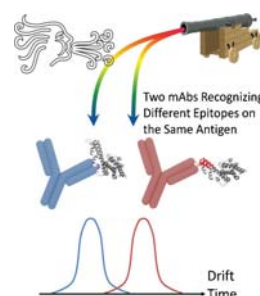
Simultaneous Improvement of Resolving Power and Signal-to-Noise Ratio Using a Modified Hadamard Transform-Inverse Ion Mobility Spectrometry Technique
Y. Hong, S. Liu, C. Huang, L. Xia, C. Shen, H. Jiang, and Y. Chu

**2508–2514**

ESI-MS of Cucurbituril Complexes Under Negative Polarity
M.A.A. Rodrigues, D.C. Mendes, V. Ramamurthy, and J.P. Da Silva

**SHORT COMMUNICATIONS****2515–2518**

Native Mass Spectrometry, Ion mobility, and Collision-Induced Unfolding Categorize Malaria Antigen/Antibody Binding
Y. Huang, N.D. Salinas, E. Chen, N.H. Tolia, and M.L. Gross

**2519–2522**

Size Exclusion Chromatography-Ion Mobility-Mass Spectrometry Coupling: a Step Toward Structural Biology
G. Van der Rest and F. Halgand

